microwaves&rf

Design for Strip-Line Band-Pass Filters

J.K. Richardson

Mon, 2013-12-09 15:46

Strip widths and gap spacings are given in graphical form for band-pass filters using symmetrical strip lines.

June, 1968

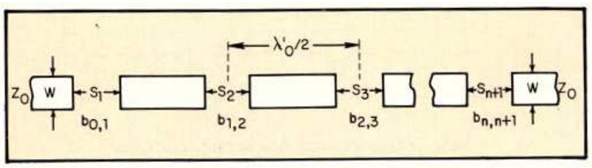

Fig. 1. **Half wavelength** end-coupled filter.

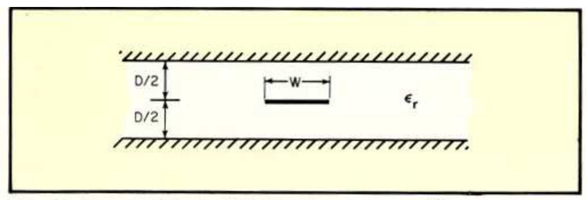

Fig. 3. **Symmetrical strip line** in cross section.

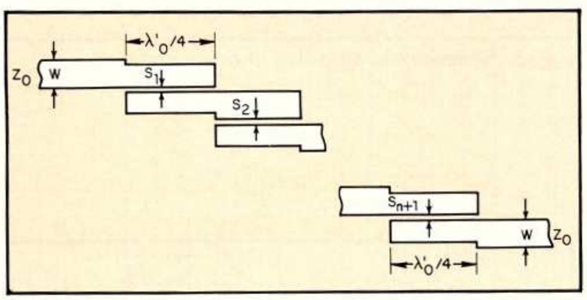

Fig. 2. **Half wavelength** side-coupled filter.

Strip-line band-pass filters can be constructed either of half-wavelength strips capacitively coupled end-to-end as shown in Fig. 1, or using parallel coupling of the half-wavelength strips as shown in Fig. 2. The advantage of parallel or side coupling over end coupling is that the filter length is reduced by approximately half, and a symmetrical frequency-response curve is obtained. The advantage of end coupling over side coupling is that the width of the filter is much less and the widths of all resonator strips are the same. The gaps between adjacent strips may be greater for side coupling but not necessarily so. If the gaps are greater, the gap tolerance for a given bandwidth is less; also, a broader bandwidth for a given tolerance can be achieved. Cohn has derived formulas which permit side-coupled filters to be accurately realized for bandwidths up to about 20% for a maximum flat response, and 30% for an equal ripple response. Other formulas are available to design end-coupled filters up to approximately the same bandwidths. The equations by Bradley and Cohn in the reference cited, are used here to construct graphs for determining band-pass filter dimensions as a function of normalized bandwidth. These graphs are for symmetrical strip line in the form shown in Fig. 3.

Design procedure

In designing these filters, first decide upon the required frequency response and the rate of attenuation beyond cut-off; then calculate the number of resonators required and the values of the equivalent low-pass prototype elements.

For the end-coupled filter, Fig. 1, it is necessary to determine the susceptance of the capacitative gaps between resonant elements; 1. as a function of strip-line geometry and permittivity of the dielectric between ground planes, and 2. as a function of the required frequency response and normalized bandwidth. Next, by eliminating the susceptance values from the two sets of equations, it is possible to obtain expressions which explicitly relate the rations S/D and W/D (See Figs. 1-3) in terms of bandwidth and frequency response. The spacings between strips will differ from one resonator to another, being least for the first and last sections.

For the side-coupled filter, Fig. 2, a similar procedure is adopted, except that instead of susceptances it is necessary to evaluate even- and odd-mode characteristic impedance of the coupled resonator strips. By eliminating the impedance values from two further sets of equations, the ratios *S/D* and *W/D* are obtained as a function of bandwidth and frequency response. As with end-coupled filters, the spacings between resonator strips will be smallest for the end sections, but the strip widths differ from one section to another. However, for bandwidths less than 1%, the value of *W/D* does not significantly differ from that obtained for the terminal strips.

A difference exists between the electrical length of the resonator strips, $\lambda'_0/2$, and the physical length for both filter types. Due to fringe fields, the electrical length is greater than the physical one, and a reduction in the latter is essential if the filter is to have an accurately positioned center frequency. Unfortunately, the formulas available to determine the necessary reduction in physical length are only approximate and have not been given in this article.

Design formulas for end-coupled filters

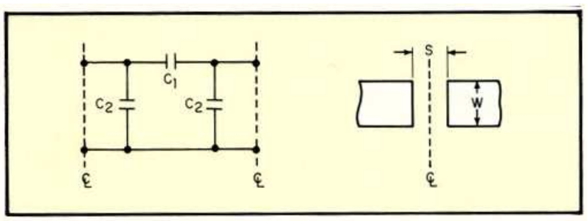

Fig. 4. Equivalent circuit of series gap in strip line (center line representation).

The equivalent circuit of a series gap in an end-coupled filter (center line representation) comprises a series capacitance, C_1, and two shunt capacitances, C_2 (Fig. 4). Following are approximate analytical relations, which relate the normalized susceptances, b_1 and b_2, associated with C_1 and C_2, to *S*, *D* and $\lambda'_0 (= \lambda_0 / \sqrt{\epsilon_r})$, the wavelength in the dielectric medium:

$$(1)\ b_1 = \frac{D}{\lambda'_0} \ln\left\{ \cosh\left(\frac{\pi S}{2D} \right) \right\}$$

and

$$(2)\ b_2 = \frac{-2D}{\lambda_0} \ln\left\{ \cosh\left(\frac{\pi S}{2D} \right) \right\}$$

Equations (1) and (2) are accurate for $W/D > 1.2$. For $S/D < 0.2$, $|b_1| > 10\,|b_2|$, and for $S/D < 0.1$, $|b_1| > 75\,|b_2|$. For the preliminary analysis of the end-coupled filter, *S/D* is assumed small enough that $|b_2|$ may be neglected.

The normalized susceptance of the (*i* + 1)-th gap of an end-coupled filter with *n* stages, $b_{i,j+1}$, may be expressed as follows:

$$(3)\ b_{i,i+1} = X_{i,i+1} / (1 - X_{i,i+1}^2)$$

where

$$(4)\ X_{0,1}=\sqrt{\frac{\pi W}{2g_0g_1}}=X_{n,n+1}$$

and

$$(5)\ X_{i,i+1}=\frac{\pi W}{2\sqrt{g_ig_{i+1}}}\left[for\ \ (n\text{-}1)\ \geq\ i\ \geq\ 1\right]$$

where

$$(6)\ \frac{W}{2}=\frac{f_2\text{-}f_1}{f_2+f_1}$$

f_1 and f_2 are the lower and upper cut-off frequencies, respectively, and

$$(7)\ \frac{2}{f_0}=\frac{1}{f_1}+\frac{1}{f_2}$$

where f_o is the center frequency of the filter and g is the normalized value of a low-pass prototype element.

Equation 1 can be rearranged into a form in which *S/D* is expressed as an explicit function of the series susceptance, b_1. From (1),

$$(8)\ \frac{\pi S}{2D}=ar\coth\left\{exp\left(\frac{b_1\lambda_0'}{D}\right)\right\}$$

and utilizing the identity

$$(9)\ ar\coth\theta=1/2\ln\left(\frac{\theta+1}{\theta\text{-}1}\right)$$

substituting for b_1 from Eq. 3, and omitting the *i* subscripts, Eq. 8 becomes

$$(10)\ \frac{S}{D}=\frac{1}{\pi}\ \ln\left\{\coth\left(\frac{\lambda_0'}{2D}\cdot\frac{X}{1\text{-}X^2}\right)\right\}$$

The value of *W/D* can be found from the equation given by Cohn for the characteristic impedance, Z_o, of a symmetrical strip line (Fig. 3):

$$(11)\quad Z_0 = \frac{94.15/\sqrt{\epsilon_r}}{\frac{W}{D} + \frac{\ln 4}{\pi}}$$

from which it follows:

$$(12)\quad \frac{W}{D} = \frac{94.15}{\sqrt{\epsilon_r}\, Z_0} - 0.441$$

Design formulas for end-coupled filters (continued)

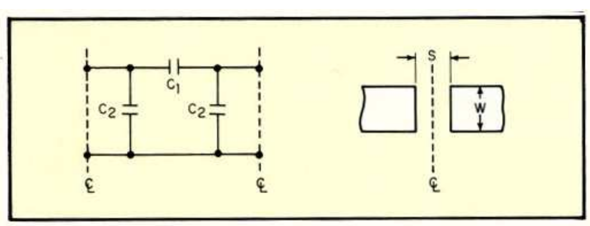

Fig. 4. Equivalent circuit of series gap in strip line (center line representation).

However, it has been assumed that b_2 is negligibly small in comparison with b_1; yet for *S/D* ≈ 0.46, $| b_1 | = | b_2 |$, and for larger values of *S/D*, $| b_2 |$ becomes increasingly greater than $| b_1 |$.

The following analysis, which accounts for b_1 and b_2, shows that Eq. 10 may be used for *S/D* as large as 0.6 accuracy of better than 1% providing $\lambda'_0/D \geq 6$.

Referring to the equivalent circuit of the series gap (Fig. 4), parameter *X* may be expressed as a function of both b_1 and b_2:

$$(13)\quad X = | \tan(\phi/2 + ar\tan b_2) |$$

where

$$(14)\quad \phi = -ar\tan(2b_1 + b_2) - ar\tan b_2$$

Therefore,

$$(15)\quad X = | \tan(\psi/2) |$$

where

$$(16)\quad \psi = -ar\tan(2b_1 + b_2) + ar\tan b_2$$

From Eq. 3, $b = X/(1-X^2)$.

Substituting from Eq. 15 and providing

$$(17)\quad \begin{aligned}&+\pi/2>\psi>-\pi/2,\\ &b=\left|1/2\tan\psi\right|\end{aligned}$$

Substituting for b_1 and b_2 from Eqs. 1 and 2 into Eq. 16, and simplifying, ψ may be expressed directly in terms of *S/D*:

$$(18)\quad \begin{aligned}\psi=&\,ar\tan\left[\frac{2D}{\lambda_0'}\ln\left\{\sinh\left(\frac{\pi S}{2D}\right)\right\}\right]\\ &-ar\tan\left[\frac{2D}{\lambda_0'}\ln\left\{\cosh\left(\frac{\pi S}{2D}\right)\right\}\right]\end{aligned}$$

Utilizing equations 17 and 18, b can be obtained as a function of *S/D* and λ'_0/D and compared with b_1 obtained from Eq. 1 as a function of the same parameters. Graphs have been prepared with the ratios b/b_1 and b_1/b plotted in Figs. 5 and 6 as functions of λ'_0/D for $1.0 \geq S/D \geq 0.1$. Note that for $S/D < 0.5$, $b > b_1$ and for $S/D > 0.6$, $b_1 < b$.

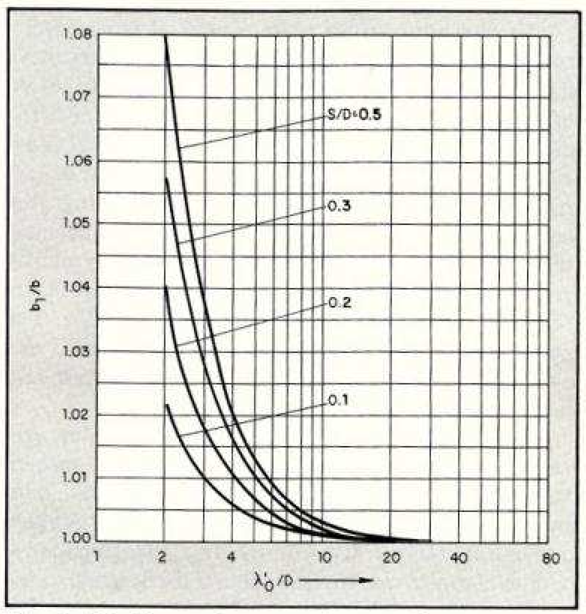

Fig. 5. Effective series susceptance ratio vs resonant wavelength/ground-plane spacing ratio.

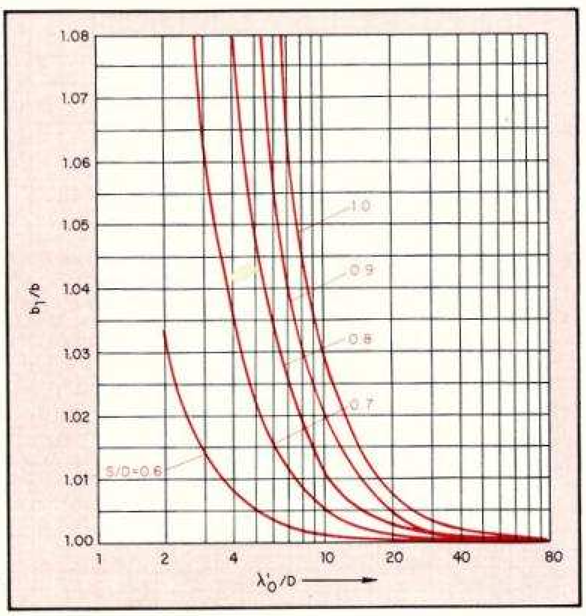

Fig. 6. Effective series susceptance ratio vs resonant wavelength/ground-plane spacing ratio.

The effect of the difference between b and b_1 on the value of strip spacing can be determined for relatively small differences by differentiating *S* with respect to b_1 in Eq. 10. Upon simplification, the following result is obtained:

$$(19)\quad \Delta S \approx \frac{D}{\pi}\cdot\frac{\Delta b}{b_1}$$

where Δ b = b ~ b_1. For b_1 $\lambda'_0/D \leq 0.5$, Eq. 19 has a maximum error of approximately 4%. By considering Figs. 5

and 6, in conjunction with Eq. 19, the error in gap spacing obtained by using Eq. 10 (which does not account for the shunt susceptances, b_2) may be determined.

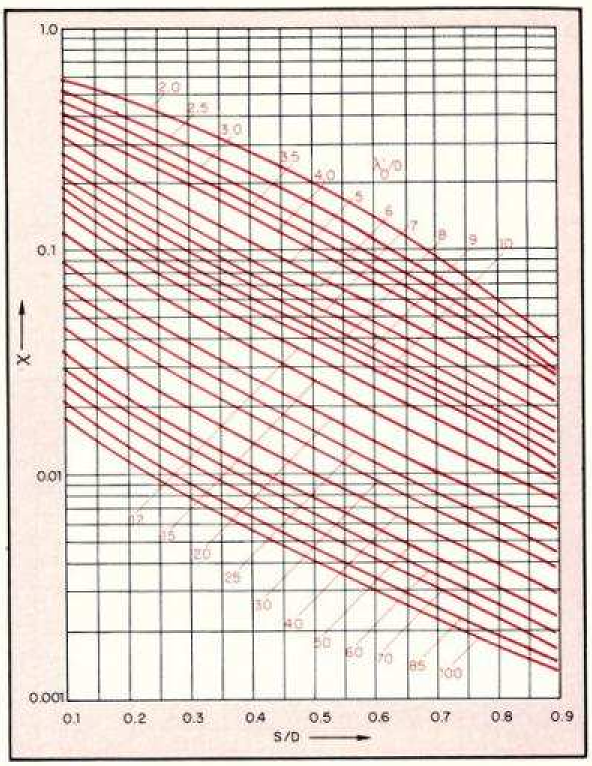

Fig. 7. **Normalized bandwidth parameter** vs strip spacing ratio for end-coupled filters.

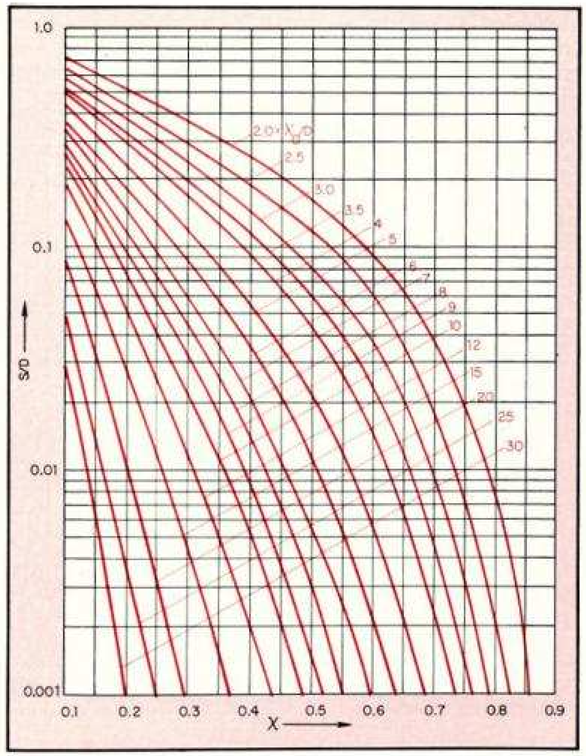

Fig. 8. **Strip spacing ratio** vs normalized bandwidth parameter for end-coupled filters.

Unfortunately, it is not possible to obtain an explicit expression for *S/D* in terms of *X*, accounting for b_1 and b_2, because of the transcendental nature of Eq. 18. Nevertheless, utilizing Eqs. 12, 15 and 18, a set of graphs has been prepared giving *X* as a function of *S/D* for $100 \geq \lambda'_0/D \geq 2$ and $1 > X > 0$ (Figs. 7 and 8) and *W/D* as a function of ϵ_r for $Z_0 = 50\ \Omega$ (Fig. 9).

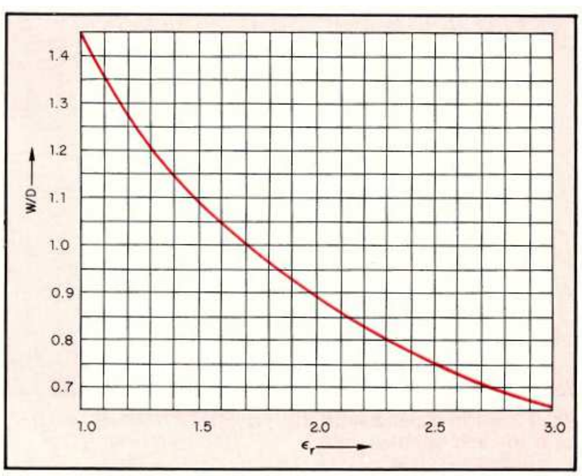

Fig. 9. **Strip width ratio** vs relative permittivity for end-coupled filters.

A lower limit of two for λ'_0/D is selected; because, if $\lambda'_0/2$ is less than *D*, higher modes will be generated, and loss by lateral radiation takes place. And from Eq. 1, b_1 is always positive if $S/D > 0$; while from Eq. 3, b is positive only if X < 1. Consequently, for Eqs. 1 and 3 to be consistent, $1 > X > 0$.

Design formulas for side-coupled filters

Design formulas for side-coupled filters

The equations which related the even and odd mode impedance, Z_{oe} and Z_{oo}, respectively, to *W/D*, *S/D* and ϵ_r have been given by Cohn (Ref. 4) and may be expressed as follows:

$$(20)\quad Z_{oe}=\frac{94.15/\sqrt{\epsilon_r}}{\frac{W}{D}+\frac{\ln 2}{\pi}+\frac{1}{\pi}\ln\left\{1+\tanh\left(\frac{\pi S}{2D}\right)\right\}}$$

and

$$(21)\quad Z_{oo}=\frac{94.15/\sqrt{\epsilon_r}}{\frac{W}{D}+\frac{\ln 2}{\pi}+\frac{1}{\pi}\ln\left\{1+\coth\left(\frac{\pi S}{2D}\right)\right\}}$$

Equations 20 and 21 are accurate to approximately 1% for $W/D = 0.35$, and become increasingly accurate for $W/D > 0.35$, and become increasingly accurate for $W/D > 0.35$.

Rearranging (20) and (21), and subtracting from the other, the ratio W/D can be eliminated and the following expression obtained:

$$(22)\quad \frac{1}{\pi}\ln\left\{\coth\left(\frac{\pi S}{2D}\right)\right\}=\frac{94.15}{\sqrt{\epsilon_r}}\left(\frac{1}{Z_{oo}}-\frac{1}{Z_{oe}}\right)$$

Solving for S/D using a similar procedure to that used to obtain Eq. 10 from Eq. 1, S/D can be expressed explicitly as a function of ϵ_r, Z_{oo} and Z_{oe}:

$$(23)\quad \frac{S}{D}=\frac{1}{\pi}\ln\left[\coth\left\{\frac{94.15}{2\sqrt{\epsilon_r}}\left(\frac{1}{Z_{oo}}-\frac{1}{Z_{oe}}\right)\right\}\right]$$

A further set of equations relating Z_{oe} and Z_{oo} to the bandwidth parameter, X, have also been given by Cohn (Ref. 2), and may be expressed as follows:

$$(24)\quad (Z_{oe})_{i,i+1} = Z_o[1+X_{i,i+1}+X_{i,i+1}^2] = Z_o\cdot(1-X_{i,i+1}^3)/(1-X_{i,i+1})$$

and

$$(25)\quad (Z_{oo})_{i,i+1} = Z_o[1-X_{i,i+1}+X_{i,i+1}^2] = Z_o\cdot(1+X_{i,i+1}^3)/(1+X_{i,i+1})$$

where $n > i > 0$ X is defined in Eqs. 4 and 5 with

$$(26)\ W = \frac{f_2 - f_1}{f_0}$$

$$(27)\ 2f_o = f_1 + f_2$$

Substituting for Z_{oe} and Z_{oo} from Eqs. 24 and 25 into Eq. 23, and eliminating the *i* subscripts and simplifying,

$$(28)\ \frac{S}{D} = \frac{1}{\pi} \ln\left[\coth\left\{ \frac{94.15}{\sqrt{\epsilon_r}\, Z_o} \cdot \frac{X(1-X^2)}{(1-X^6)} \right\} \right]$$

As the maximum permissible value of X is 0.5 (Ref. 3), the term X^6 can usually be neglected.

Substituting for *S/D* from Eq. 28 into Eq. 20, and for Z_{oe} from Eq. 24, an explicit expression for *W/D* is obtained:

$$(29)\ \frac{W}{D} = \frac{94.15}{\sqrt{\epsilon_r}\, Z_o} / (1+X+X^2) - \frac{1}{\pi} \ln\{2(1+1/\psi)\}$$

where

$$(30)\ \ln\psi = \frac{94.15}{\sqrt{\epsilon_r}\, Z_o} \cdot \frac{2(1-X^2)}{(1-X^6)}$$

For very narrow bandwidths, corresponding to $X < 0.01$, *W/D* can be taken as equal to that of the terminating strips, as given by Eq. 15 or graphically in Fig. 9. Moreover, both the X^2 and X^6 terms can be neglected in Eq. 28 for narrow bandwidths.

Hence, ratios *S/D* and *W/D* can be found for side-coupled filters as a function of the parameters X, ϵ_r, and Z_o. Additional graphs have been prepared (Figs. 10-12) in which *S/D* and *W/D* are plotted as functions of X for values of ϵ_r and for $Z_o = 50\Omega$.

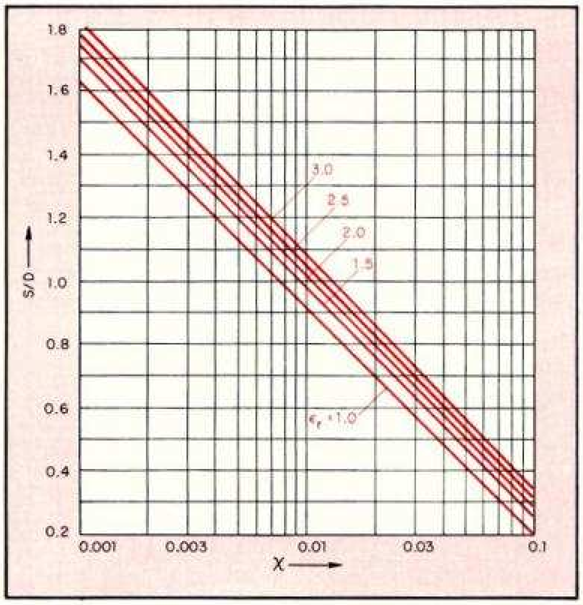

Fig. 10. Strip spacing ratio vs normalized bandwidth for side-coupled filters.

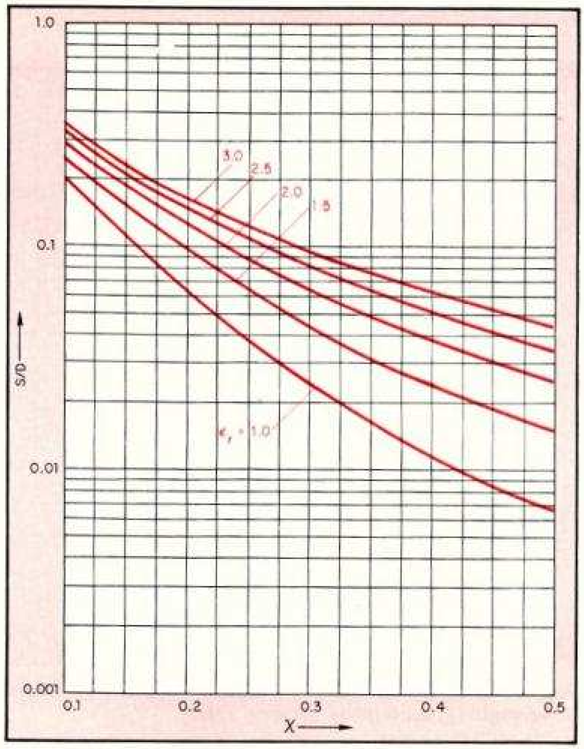

Fig. 11. Strip spacing ratio vs normalized bandwidth parameter for side-coupled filters.

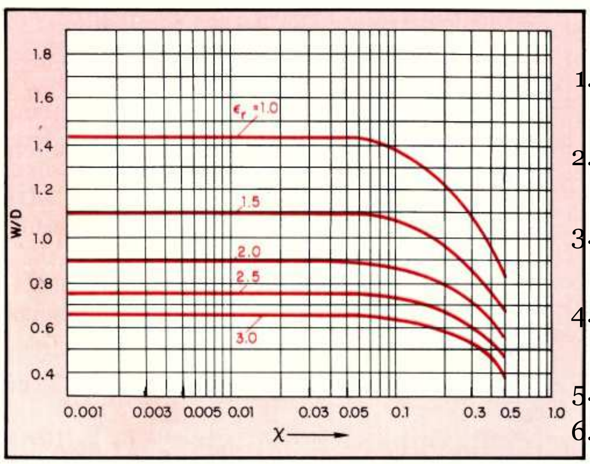

Fig. 12. Strip width ratio vs normalized bandwidth parameter for side-coupled filters.

References

1. E.G. Bradley, "Design and Development of Strip Line Filters," *IRE Trans. MTT,* (April, 1956).
2. S.B. Cohn, "Parallel Coupled Strip Line Resonator Filters," *L'Onde* [France], (October, 1957).
3. J.K. Richardson, "Gap Spacing for End Coupled and Side Coupled Band Bass Filters," *IEEE Trans. MTT*. (June, 1967).
4. S.B. Cohn, "Shielded Coupled Strip Transmission Line," *IRE Trans. MTT*, (October, 1957).
5. E.G. Bradley, *op.cit*.
6. S.B. Cohn, "Direct Coupled Resonator Filters," *Proc. IRE*, (February, 1957).
7. H.M. Altschuler and A.A. Oliner, "Discontinuities in the Centre Conductor of Symmetric Strip Transmission Line," *IRE Trans. MTT,* (May, 1960).
8. G.L. Matthew, L. Young and E.M.I. Jones, *Microwave Filters, Impedance-Matching Networks, and Coupling Structures*, (McGraw-Hill Book Co., 1964).
9. E. Rubins, W. Fromm and H. Keen, "New Techniques for High Q Microwave Components," *IRE Convention Record, Part 8*, (1954).

Source URL: http://mwrf.com/rf-classics/design-strip-line-band-pass-filters